Philosophical Magazine
Vol. 93, No. 28-30, 19 October 2013, 3417–3429

RESEARCH ARTICLE

Carbon in Cubic and Tetragonal Ferrite

H. K. D. H. Bhadeshia

University of Cambridge, Materials Science and Metallurgy, U. K.
(*Received 00 Month 200x; final version received 00 Month 200x*)

It is generally assumed that the phase diagrams and equilibrium thermodynamic data that apply to the conventional Fe-C system, also are relevant to the case where supersaturated ferrite is in contact with austenite. It seems that this may not be correct, since a change in the symmetry of the ferrite unit cell in the presence of excess carbon has the potential to alter the nature of the phase equilibrium. The implications of these discoveries are presented in the context of the early recognition by Cottrell and co-workers, of the importance that should be attached to the tetragonal symmetry of the octahedral interstices in the ferritic allotrope of iron.

Keywords: interstitial carbon; cubic ferrite; tetragonal ferrite; thermodynamics; diffusion; bainite

1. Introduction

The key mechanical consequences of carbon in body-centred cubic iron were placed on a firm foundation by Cottrell and Bilby [1] but there are other effects that are less well-known, some which have only just been revealed. They control the thermodynamic and kinetic properties of Fe-C alloys and influence the interpretation of modern data and the design of some of the most exciting of steels. I hope in this paper to place the essential concepts in an order that stimulates further research and alloy development. Alan Cottrell once asked the rhetorical question "Will anybody ever use metals and alloys again?" [2], and as was his habit, he kept me supplied with reprints of his work, which left me in no doubt about the answer!

2. Symmetry of Interstices

The carbon atom is small in comparison with iron, so consistent with the Hume-Rothery rules, it occupies the interstices between the iron atoms within the crystalline lattice. There are many allotropic forms of iron, but the most common are illustrated in Fig. 1 together with the corresponding hard-sphere models of the octahedral and tetrahedral interstices. A close examination shows that the body-centred cubic lattice is special, in that neither of the interstices illustrated are regular. In the octahedral case, one of the axes has a length a_α, the lattice parameter of ferrite, whereas the other two are along the $< 1\ 1\ 0 >$ directions with length $\sqrt{2}a_\alpha$. The shortest axis has four-fold symmetry so a vacant octahedral site in ferrite has tetragonal symmetry $\frac{4}{m}\ \frac{2}{m}\ \frac{2}{m}$. As a result, placing a carbon atom in the

*Corresponding author. Email: hkdb@cam.ac.uk

ISSN: 1478-6435 print/ISSN 1478-6443 online

DOI: 10.1080/14786435.2013.775518
http://www.informaworld.com

octahedral site causes essentially a uniaxial distortion which leads to a *reduction* in the tetragonality of the interstitial site, though an increase in the tetragonality of the original cubic lattice if carbon atoms act in concert and align parallel to one of the cube edges.

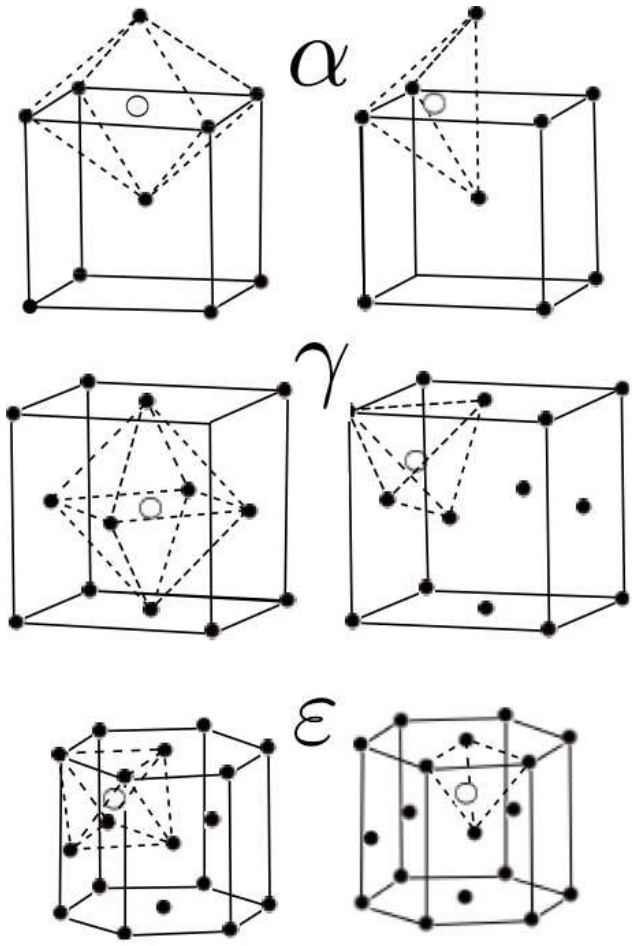

Figure 1. Schematic representation of the octahedral and tetrahedral interstices in ferrite (α), austenite (γ) and hexagonal iron (ε). The interstices are represented by open circles together with their coordination polyhedra.

The tetrahedral interstice in ferrite is also irregular with two edges parallel to $< 1\ 0\ 0 >$ directions, and the remaining four being along $< 1\ 1\ 1 >$ directions, with lengths a_α and $a_\alpha\sqrt{3}/2$ respectively. The lines joining the corners of the tetrahedron to its centre are of the form $< 2\ 1\ 0 >$.

The largest atom that can fit without distortion in an octahedral site is $a_\alpha(1/2 - \sqrt{3}/4) = 0.067a_\alpha$, in contrast to $a_\alpha(\sqrt{5}/4 - \sqrt{3}/4) = 0.126a_\alpha$ for the tetrahedral hole. And yet, carbon atoms predominantly occupy the octahedral sites, because distortion of the tetrahedral interstice is more uniform with all four "bonds" stretched, whereas it is primarily the cube edge which accommodates the distortion in the octahedral case. The strain energies for the two cases when Poisson's effects are neglected are proportional to [3]:

$$U_O \propto 2(r_i - r_o)^2 E_{100}$$

where r_i is the interstitial-atom radius, r_o is the radius of the undistorted hole and E is the Young's modulus along the crystallographic direction identified in the

subscript. For the tetrahedral site,

$$U_{Te} \propto 4(r_i - r_o)^2 E_{210}$$

so for $r = 0.08$ nm, $U_{Te}/U_O = 1.38$. More recent calculations suggest that there is a substantial difference in the chemical energy of solution between the octahedral and tetragonal sites, which makes the former interstice the favoured site for carbon atoms [4].

Cottrell and Bilby appreciated the need to deal with the tetragonal symmetry of the distortion caused by the carbon atom when addressing its interaction with edge dislocations. But to avoid complexity they considered only the hydrostatic strain caused by carbon in order to calculate the interaction energy, since the orientation of the dislocation relative to the tetragonal strain can then be neglected. This amounted to treating carbon as if it is a substitutional solute, with only a weak interaction with screw dislocations. The approximation is better explained by comparing carbon in austenite with that in ferrite. The octahedral interstice in austenite is regular (Fig. 1) so carbon causes an isotropic expansion. The effect of carbon on the hardening of austenite is therefore much weaker than the dramatic strengthening it causes in ferrite, even if the relatively large size of the interstice in austenite is taken into account. A tetragonal strain can interact strongly with both the shear and dilatational components of the dislocation strain field [5, 6], whereas it is only the dilatational strain that features in austenite.

3. Thermodynamic Stability

Given the misfit between the carbon atom and the interstices in ferritic iron, it is not surprising that the solubility of carbon in ferrite, whether it is in equilibrium with austenite, cementite or graphite, is very small. As will be seen later, the maximum value is around 0.02 wt% when the ferrite is in equilibrium with austenite. It is of course possible to force excess carbon into the ferrite by quenching high-carbon austenite from an elevated temperature, in which case there are important consequences that bear further discussion.

3.1. *Ordering due to transformation*

There is one octahedral interstice per iron atom in austenite, but three in the case of ferrite or martensite. The deformation which carries the austenite into martensite is known as the Bain strain [7], Fig. 2, with compression along the z axis and uniform expansion along the x and y axes. Suppose that three carbon atoms are located in the octahedral interstices marked 'o' in the austenite, then as a consequence of the Bain strain, they would all end up in just one of the three sub-lattices of octahedral interstices in the resultant body-centred cell, making it tetragonal. It is this ordering which leads to the tetragonality of martensite in steels.

Like any ordering phenomenon, the carbon atoms will tend to randomise if the temperature is above that for Zener ordering [8], in which case, the martensite will not be tetragonal, but cubic. However, this is an after-effect, in which carbon atoms initially ordered by the Bain strain would tend to disorder assuming sufficient mobility.

It is important to note that the diffusionless transformation of austenite containing carbon in the first instance necessarily leads to a body-centred tetragonal lattice.

It therefore becomes legitimate to enquire whether the routine use of the thermodynamic data for cubic ferrite, to calculate equilibrium with austenite, is correct for cases where the ferrite inherits a large concentration of carbon from the austenite. The long-standing anomalies described in the next section might be attributable to a failure to consider *ab initio* the equilibrium between the body-centred tetragonal ferrite and austenite.

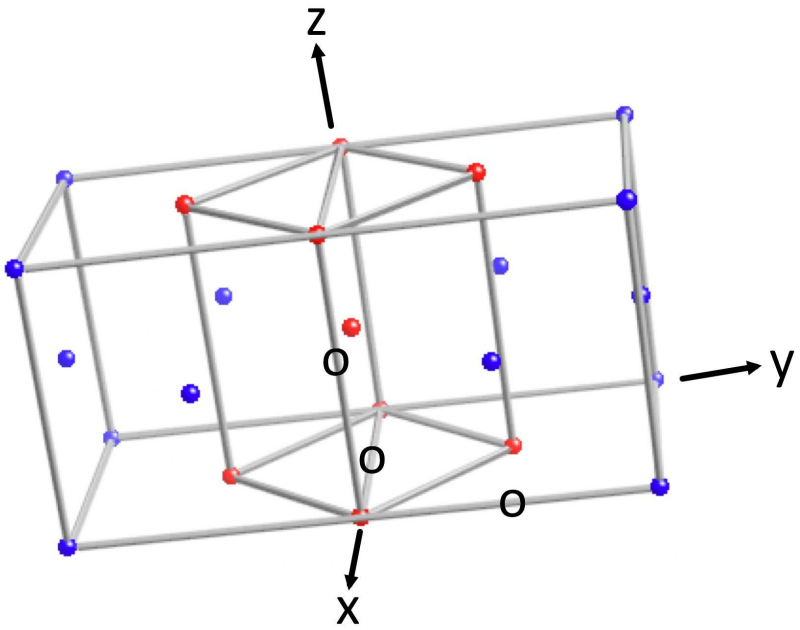

Figure 2. The red and blue atoms together represent two unit cells of face-centred cubic austenite. The ones marked red also form a body-centred tetragonal (bct) cell of austenite. To transform the latter into a body-centred cubic cell, the bct cell is compressed along the vertical axis and expanded uniformly along the horizontal axes. This is the Bain strain. The locations marked 'o' represent octahedral interstices on the cube edges of the austenite, where carbon may reside.

3.2. *Excess carbon in bainitic ferrite*

An alloy system based on iron has recently been created, containing an incredibly large density of interfaces, generated by heat-treatment alone [9, 10]. The resulting structure consists of a mixture of slender platelets of bainitic ferrite, just 20-40 nm in thickness, embedded in a matrix of carbon-enriched austenite. The rate at which this structure evolves is slow by conventional standards, but this permits engineering components to be made which are large in all three dimensions, with uniform properties throughout. Many hundreds of tonnes have been manufactured and the material is commercially available in large quantities [11]. [1] Nanostructured steels like this have not fared well in the past because the ability to work harden, and

[1]The term 'nanostructure' has unfortunately become a generic reference to a wide range of grain and precipitate structures, to the extent that it is often misleading and taken to represent structures far coarser than the adjective would imply [12]. We define it to represent cases where the interfacial area per unit volume, S_V, is large enough to make the governing length scale $\overline{L} = 2/S_V$ comparable to the narrower dimensions of carbon nanotubes, i.e., of the order 20-50 nm.

hence to avoid plastic instabilities becomes vanishingly small as the grain size is reduced [13]. However the carbon-rich austenite undergoes stress-induced martensitic transformation which introduces the required work hardening capacity, thus enabling ductility in spite of the strength which is in excess of 2 GPa. It is interesting that Cottrell [14] studied the transformation plasticity associated with bainite back in 1945!

The discovery has sparked a great deal of research in academia and industry, using some of the most modern experimental techniques available. In the present context of carbon in ferrite, there are a few important anomalies which remain to be explained.

The mechanism of the bainite reaction is summarised in Fig. 3; the transformation is diffusionless in the first instance, but carbon subsequently partitions into the residual austenite, where it remains if the silicon concentration is sufficiently large [15], or precipitates as cementite.

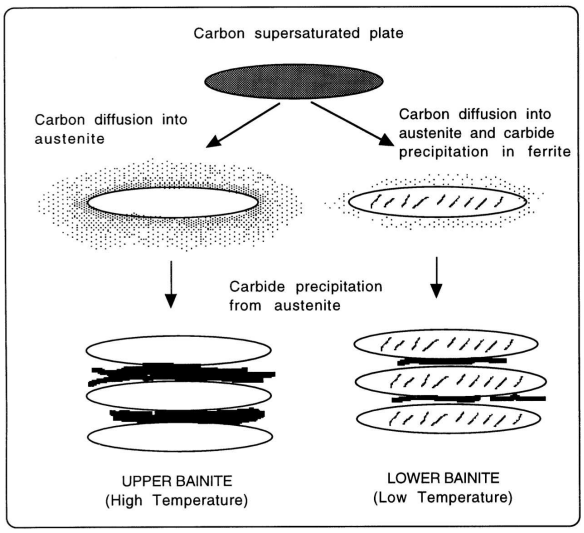

Figure 3. Bainite inherits the carbon concentration of the austenite, but some of the carbon may subsequently partition into the residual austenite, or precipitates as cementite depending on the chemical composition of the steel [16].

The maximum solubility of carbon in ferrite that is in equilibrium with austenite is a little greater than 0.02 wt% at a temperature of about 600 °C due to the retrograde shape of the $\alpha/\alpha + \gamma$ phase boundary [17, 18]. It has been known from direct measurements using the atom-probe technique, that bainitic ferrite is supersaturated with an excess of carbon [19–22]. This carbon fails to partition into the residual austenite in spite of the fact that the process is not limited by atomic mobility [23]. In fact, the accumulated evidence demonstrates that the carbon inherited by bainitic ferrite is reluctant to partition into the residual austenite in spite of prolonged heat treatment [19, 24–28]. The early interpretations of these observations attributed this reluctance of the carbon to partition on the presence of dislocations which trap the solute, i.e., the famous Cottrell atmospheres [1, 29, 30]. However, recent meticulous work has shown conclusively using the most advanced atom-probe technique, that large quantities of excess carbon remain in defect-free solid solution [31, 32]. What is the explanation for the reluctance of the dissolved carbon in the bainitic ferrite to partition into the residual austenite?

This question is of course based on the assumption of the equilibrium between cubic ferrite and austenite, i.e., the conventional Fe-C phase diagram. However, if the bainite inherits the composition of the austenite, then it will be body-centred

tetragonal and the conventional phase diagram should no longer be applicable. In the absence of thermodynamic data for body-centred tetragonal iron, Jang et al. [33] used *ab initio* methods to calculate the required data, and subsequently incorporated them into routine phase diagram calculation procedures. The results are shown in Fig. 4 where it is clear that the solubility of carbon in tetragonal ferrite in equilibrium with austenite is much larger than that for cubic ferrite.

It is possible therefore, that the change in symmetry of the ferrite may explain the observed reluctance for the "excess" carbon present in bainitic ferrite to partition into the residual austenite despite prolonged heat treatment. The tetragonaility may exist over a long range, but the possibility of a domain structure, such as that found in minerals which undergo cubic to tetragonal transitions, should not be ruled out. Experiments are now in progress to characterise this tetragonality [34].

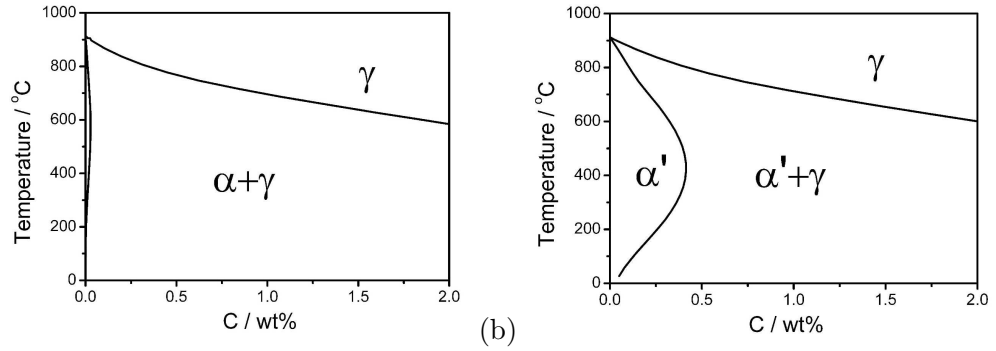

Figure 4. Binary phase diagrams of the Fe-C system allowing (a) equilibrium between body-centred cubic ferrite and austenite, (b) between body-centred tetragonal ferrite and austenite [33].

In summary, the most exciting discovery from the atomic resolution studies is definitive proof that the excess carbon in bainitic ferrite is not just found at defects, but is present in solid solution [31, 32]. This is an insightful result which can only be explained by the displacive transformation mechanism for bainite. Furthermore, this result is consistent with a new Fe-C phase diagram in which the equilibrium between *tetragonal* ferrite and austenite is considered [33]. Subsequent to the work of Jang and co-workers [33], similar calculations have been published [35] that show how strain fields that exist in deformed pearlite increase the solubility of carbon in ferrite.

4. Kinetics of Carbon in Ferrite

Although a variety of regular solution models and their adaptations are used in calculating phase equilibria with ferrite, they rely on formalisms for the easy computation of phase diagrams rather than on rigorous representations of the nature of carbon distribution in ferrite. It is likely that there is a strong repulsion between carbon atoms located at nearest neighbour octahedral interstices in ferrite, although measured thermodynamic data which necessarily are from very dilute solutions, may not be accurate enough to establish this [36, 37]. However, first principles calculations [38] have proven that this repulsion exists and is large, with interstices spaced one lattice parameter apart on parallel cell-edges being favoured. This of course, is consistent with the formation of tetragonal martensite in steel. However, it is not always safe to assume that carbon atoms occupy only the octahedral interstices.

4.1. *Diffusion in Cubic Ferrite*

Combined diffusion data covering some fourteen orders of magnitude in the diffusion coefficient show that the diffusion coefficient does not strictly follow an Arrhenius relationship over a large range of temperatures, with perceptible deviations from the straight line on a plot of $\ln\{D\}$ versus T^{-1}, Fig. 5 [39]. This nonlinear

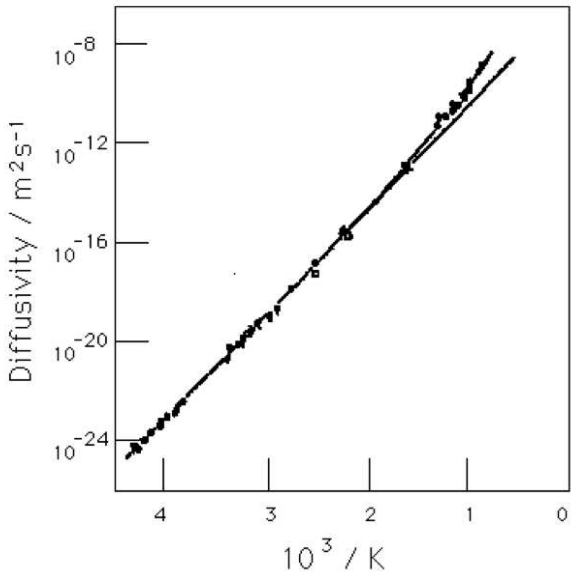

Figure 5. The diffusion data for carbon in ferrite, showing deviations from the Arrhenius behaviour. After McLellan et al. [39].

behaviour has its origin in the changing occupancy, as a function of temperature, of the octahedral (O) and tetrahedral (Te) sites [39]. Although the fraction of carbon atoms that reside in the tetrahedral sites is quite small (about one atom in a thousand at high temperatures), the deviation from linearity is nevertheless significant because the activation energy for jumps between adjacent tetrahedral sites is relatively small.

Let the activation free energies for the $O \rightarrow Te$ and $Te \rightarrow O$ jumps be G^*_O and G^*_{Te} respectively. The jump probability for $O \rightarrow Te$ is proportional to $\beta_{Te} \exp\{-G^*_O/RT\}$, where β_{Te} is the number of tetrahedral sites per solvent atom, into which a carbon atom originally in the octahedral site can jump. It follows that the probable ratio of the number of occupied tetrahedral sites (N_{Te}) to occupied octahedral sites is given by [39]:

$$\frac{N_{Te}}{N_O} = \frac{\beta_O}{\beta_{Te}} \exp\left\{-\frac{G^*_{Te} - G^*_O}{RT}\right\}$$

Since $\beta_O = 3$ and $\beta_{Te} = 6$, the fraction ϕ_O of carbon atoms in the octahedral sites is:

$$\phi_O = 1 - \left(\frac{3}{6} \exp\left\{-\frac{G^*_{Te} - G^*_O}{RT}\right\} + 1\right)^{-1}$$

Given the distribution of carbon atoms amongst the octahedral and tetrahedral sites, it becomes possible to consider the combined effect of the diffusion paths between near neighbour interstices:

(1) An atom in a tetrahedral site can jump either into an adjacent Te site, or an O site.
(2) Given that direct jumps between neighbouring octahedral sites must involve passage through a tetrahedral site, a third diffusion path is $O - Te - O$.

The overall diffusion coefficient D is then given by:

$$D = \phi_O D_{O-Te-O} + (1 - \phi_O)\phi_{Te-Te} D_{Te-Te} + (1 - \phi_O)(1 - \phi_{Te-Te}) D_{Te-O-Te}$$

where ϕ_{Te-Te} is the fraction of carbon atoms in the tetrahedral sites which jump by the $Te \rightarrow Te$ route. By fitting this equation to the experimental data, McLellan et al. were able to explain the nonlinear behaviour in the Arrhenius plot, assuming the parameter values given in Table 1.

Table 1. Parameters describing the diffusion of carbon in ferrite. The first set of parameters is due to McLellan, Rudee and Ishibachi (1965), derived by fitting the dual-occupancy model to experimental data. The value of $D_{o,Te-Te}$ was slightly corrected by Condit and Beshers (1967). The second set is calculated by Beshers (1965). D_o is the pre-exponential in the equation $D = D_o \exp\{-Q/RT\}$, where Q is an activation energy (enthalpy) and G^* the activation free energy. U_O is the energy of a carbon atom in an octahedral site.

Dual Occupancy Model	
$D_{o,O-Te-O}$	$3.3 \times 10^{-7}\,\mathrm{m^2\,s^{-1}}$
$D_{o,Te-Te}$	$2.6 \times 10^{-}4\,\mathrm{m^2\,s^{-1}}$
Q_{O-Te-O}	$80.8\,\mathrm{kJ\,mole^{-1}}$
Q_{Te-Te}	$61.5\,\mathrm{kJ\,mole^{-1}}$
$G^*_{Te} - G^*_O$	$30.1 + 4.4RT\,\mathrm{kJ\,mole^{-1}}$
ϕ_{Te-Te}	0.86
Calculations using Elasticity Theory	
Q_{O-O}/U_O	1
Q_{O-Te}/U_O	0.69
Q_{Te-O}/U_O	0.31
Q_{Te-Te}/U_O	0.91

The data in Table 1 show that the two models give a different trend for the activation energy for jumps between tetrahedral sites when compared with the $O - Te - O$ route. Beshers predicts the latter route to have the smallest activation energy, whereas McLellan et al. deduce a lower value for the $Te - Te$ jumps. A recent estimate using first principles calculations to deduce the activation energy for the octahedral to tetrahedral jump [40] is in fact wrong because the energy difference for a carbon atom in these two sites is misinterpreted as an activation energy. These are therefore, unresolved issues.

4.2. *Diffusion in Tetragonal Ferrite*

The octahedral interstices for which the four-fold axis happens to be parallel to the c-axis of the body-centred tetragonal lattice are slightly expanded, whereas those whose tetrads lie on the basal plane of the bct lattice are contracted relative to the cubic lattice (Fig. 6a). During diffusion it may be necessary for the carbon atom to jump into the less favoured, contracted octahedrons. The diffusion of carbon in tetragonal ferrite is therefore expected to be slower than in ferrite [41].

For the bct lattice, Zener [42–44] has estimated the energy U_C to move a carbon atom from a preferred to an unfavourable adjacent octahedral site. The effect of

an applied tensile stress along [1 0 0] in a single-crystal sample of the random solution is to cause a strain ϵ with a corresponding increase in the internal energy by $\frac{1}{2}E_{100}\epsilon^2$, where E_{100} is the elastic modulus for tensile deformation along the [1 0 0] direction. If the random solution is now completely ordered, then the total change in energy is:

$$\frac{1}{2}E_{100}\epsilon^2 - \frac{2}{3}c_1U_C$$

since only two-thirds of the carbon atoms redistribute in the transition from the random to the ordered state. The concentration c_1 is the number of carbon atoms per unit volume. Stress is not needed to maintain the strain ϵ if the derivative of the energy with respect to the strain is zero,

$$E_{100}\epsilon - \frac{2}{3}c_1\frac{dU_C}{d\epsilon} = 0.$$

Bearing in mind that U_C is the change in energy on moving a carbon atom from a preferred to an unfavourable site, and that ϵ is due to an externally applied stress, it may be assumed that for small ϵ,

$$U_C = E_{100}\epsilon_*\epsilon$$

where ϵ_* is the strain caused by the transfer of one carbon atom per unit volume between the two kinds of sites. For a fully ordered sample, the strain $\epsilon = \frac{2}{3}c_1\epsilon_*$, so that

$$U_C = \frac{2}{3}E_{100}\epsilon_*^2c_1$$

On substituting $E_{100} = 1.25 \times 10^{11}\,\mathrm{N\,m^{-2}}$, $\epsilon_* = 1.176 \times 10^{-29}$, $c_1 = (N_a/V_m)x_1$ we see that $U_C = 9.9 \times 10^{-19}x_1\,\mathrm{J}$.

Hillert (1959) argued that the effect of introducing tetragonality to the cubic lattice is to lower the energy of the preferred site by $\frac{1}{2}U_C$ and to raise that of the contracted site by the same amount (Fig. 6b). In this way, the height of the barrier from the preferred site is increased by $\frac{1}{2}U_C$, so that the jump probability from that site is correspondingly reduced by a factor $\exp\{-N_aU_C/2RT\}$; N_a is Avogadro's number. Assuming that long-range diffusion is dominated by the largest barrier, he concluded that

$$D_{\alpha'} \simeq D_\alpha \exp\{-N_aU_C/2RT\}$$

where α and α' refer to ferrite and bct-ferrite respectively. The diffusivity in bct-ferrite should decrease exponentially with its carbon concentration assuming that the bct-ferrite is tetragonal at the temperature and concentration of interest.

It is interesting to mention here another kind of transport phenomenon which is now undergoing a revival in the context of complex bearings. Bearings have to be hard in order to sustain repeated contact stresses; as a result their most common microstructure consists of partially tempered martensite with a hardness in excess of 60 HRC [46]. During service, circumferential bands which etch dark are created below the contact surface [47–49]; these are regions of over-tempered martensite and represent a form of damage. The tempering here is caused not by thermal activation, but by an ill-understood phenomenon known as *mechanical tempering* [50]. The process definitely involves the migration of carbon, probably by

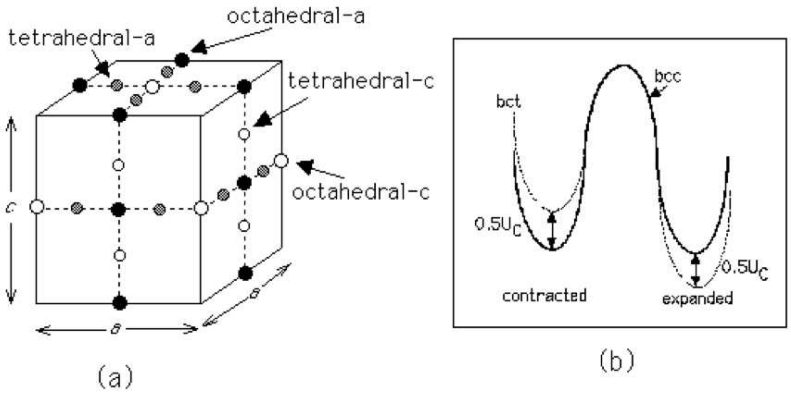

Figure 6. Octahedral and tetrahedral sites on the surface of a body-centred tetragonal cell [45]. The c/a ratio has been exaggerated for the purposes of illustration. Hollow circles represent expanded holes, whereas filled circles represent those that are contracted, the deformations being defined with respect to the cubic lattice. (b) The influence of tetragonality on the barrier to diffusion between adjacent octahedral sites.

the mechanism proposed originally by Cottrell and Jawson [29] in which the carbon atmospheres around dislocations can translate as long as the dislocations move sufficiently slowly. The cyclic movement of dislocations during repeated reversals of contact loads can therefore transport the carbon to pre-existing carbides, leading them to coarsen and hence causing the martensite to soften. The theory behind this mechanical tempering is now being developed in detail [51].

5. Concluding Remarks

Of all the forms of iron, ferrite has always been the most intriguing with its stability extending over two temperature ranges between melting and ambient temperatures, with its magnetic transitions mistaken to represent another allotrope β, and because its expansion coefficient is actually less than that of the close-packed austenite. In this paper I have emphasised the importance of the symmetry of the octahedral interstices, and how the equilibrium phase diagram for the iron-carbon system would change if the unit cell itself adopts a tetragonal form.

There are a number of anomalous measurements which indicate that carbon is reluctant to partition from ferrite which is supersaturated, into austenite with which it is in contact, assuming that the supersaturation is defined with respect to the conventional Fe-C phase diagram. However, there is no difficulty in explaining observations dating back to 1981, if the ferrite inherits the carbon concentration of the austenite, hence assumes a tetragonal unit cell as required by the Bain strain, and therefore adopts the new phase diagram resulting from equilibrium between the tetragonal ferrite and austenite.

In many technological developments [52–54, e.g.], heat-treatments are conducted to enrich austenite by partitioning from supersaturated ferrite. The models used to define the heat-treatments may need to be reassessed to account for the tetragonality of the ferrite. Similar conclusions apply to the theory of partitioning [23, 55, 56].

It is possible also to speculate how the tetragonal ferrite could be created without the presence of carbon. A number of appropriate iron-based alloy systems exist, as reviewed by Christian [57]. These could form the basis of new studies given the insight from first principles calculations.

I would like to make a finishing comment. My perception is that there are a few scholars whose papers are consistently pregnant with meaning and yet are written to excite and thrill. Alan Cottrell's publications continue to fire my imagination

and I have yet to study them all.

References

[1] A. H. Cottrell, B. A. Bilby, Proc. Physics Society A 62 (1949) 49–62.
[2] A. H. Cottrell, in: A. Briggs (Ed.), The Science of New Materials, pp. 4–31.
[3] D. N. Beshers, Journal of Applied Physics 36 (1965) 290–300.
[4] D. H. R. Fors, G. Wahnstr´om, Physical Review B 77 (2008) 132102.
[5] A. W. Cochardt, G. Shoek, H. Wiedersich, Acta Metallurgica 3 (1955) 533–537.
[6] R. L. Fleischer, Acta Metallurgica 10 (1962) 835–842.
[7] E. C. Bain, Trans. AIME 70 (1924) 25–46.
[8] J. C. Fisher, J. H. Hollomon, D. Turnbull, Metals Transactions 185 (1949) 691–700.
[9] F. G. Caballero, H. K. D. H. Bhadeshia, Current Opinion in Solid State and Materials Science 8 (2004) 251–257.
[10] H. K. D. H. Bhadeshia, Proceedings of the Royal Society of London A 466 (2010) 3–18.
[11] T. S. of State for Defence, H. K. D. H. Bhadeshia, C. Mateo, P. Brown, Intellectual Property Office, London, Patent number GB2462197 (2010).
[12] H. K. D. H. Bhadeshia, Science and Technology of Advanced Materials ? (2013) In press.
[13] A. A. Howe, Materials Science and Technology 16 (2000) 1264–1266.
[14] A. H. Cottrell, Journal of the Iron and Steel Institute 151 (1945) 93P–104P.
[15] E. Kozeschnik, H. K. D. H. Bhadeshia, Materials Science and Technology 24 (2008) 343–347.
[16] M. Takahashi, H. K. D. H. Bhadeshia, Materials Science and Technology 6 (1990) 592–603.
[17] H. I. Aaronson, H. A. Domian, G. M. Pound, TMS–AIME 236 (1966) 753–767.
[18] H. K. D. H. Bhadeshia, Metal Science 16 (1982) 167–169.
[19] H. K. D. H. Bhadeshia, A. R. Waugh, Acta Metallurgica 30 (1982) 775–784.
[20] H. K. D. H. Bhadeshia, A. R. Waugh, in: H. I. Aaronson, D. E. Laughlin, R. F. Sekerka, C. M. Wayman (Eds.), Solid-Solid Phase Transformations, TMS–AIME, Warrendale, Pennsylvania, USA, 1982, pp. 993–998.
[21] I. Stark, G. D. W. Smith, H. K. D. H. Bhadeshia, in: G. E. Lorimer (Ed.), Phase Transformations '87, Institute of Metals, London, U.K., 1988, pp. 211–215.
[22] I. Stark, G. D. W. Smith, H. K. D. H. Bhadeshia, Metallurgical transactions A 21 (1990) 837–844.
[23] H. K. D. H. Bhadeshia, in: G. W. Lorimer (Ed.), Phase Transformations '87, Institute of Metals, London, U.K., 1988, pp. 309–314.
[24] M. Peet, S. S. Babu, M. K. Miller, H. K. D. H. Bhadeshia, Scripta Materialia 50 (2004) 1277–1281.
[25] F. G. Caballero, M. K. Miller, S. S. Babu, C. Garcia-Mateo, Acta Materialia 55 (2007) 381–390.
[26] C. Garcia-Mateo, M. Peet, F. G. Caballero, H. K. D. H. Bhadeshia, Materials Science and Technology 20 (2004) 814–818.
[27] F. G. Caballero, M. K. Miller, A. J. Clarke, C. Garcia-Mateo, Scripta Materialia 63 (2010) 442–445.
[28] I. B. Timokhina, X. Y. Xiong, H. Beladi, S. Mukherjee, P. D. Hodgson, Materials Science and Technology 27 (2011) 739–741.
[29] A. H. Cottrell, M. A. Jawson, Proceedings of the Royal Society A 199 (1949) 104–114.
[30] A. H. Cottrell, Progress in Metal Physics 4 (1953) 205–264.
[31] F. G. Caballero, M. K. Miller, C. Garcia-Mateo, J. Cornide, Journal of Alloys and Compounds (2012) doi:10.1016/j.jallcom.2012.02.130.
[32] F. G. Caballero, M. K. Miller, C. Garcia-Mateo, J. Cornide, M. J. Santofimia, Scripta Materialia 67 (2012) 846–849.
[33] J. H. Jang, H. K. D. H. Bhadeshia, D. W. Suh, Scripta Materialia 68 (2012) 195–198.
[34] C. Smith, private communication, tetragonal bainitic ferrite, University of Cambridge, 2013.
[35] G. A. Nematollahi, J. von. Pezold, J. Neugebauer, D. Raabe, Acta Materialia . (2013) http://dx.doi.org/10.1016/j.actamat.2012.12.001.
[36] H. K. D. H. Bhadeshia, Metal Science 14 (1980) 230–232.
[37] H. K. D. H. Bhadeshia, Journal of Materials Science 39 (2004) 3949–3955.
[38] J. Chen, Ternary Quasichemical Thermodynamics and First-Principles Calculations (Fe-C), Master's thesis, University of Cambridge, http://www.msm.cam.ac.uk/phase-trans/2004/chen.thesis.pdf, U. K., 2004.
[39] R. B. McLellan, M. L. Rudee, T. Ishibachi, Trans. A.I.M.E. 233 (1965) 1939–1943.
[40] D. E. Jiang, E. A. Carter, Physical Review B 67 (2003) 214103.
[41] B. S. Lement, M. Cohen, Acta Metallurgica 4 (1956) 469–476.
[42] C. Zener, Trans. Am. Inst. Min. Metall. Engng. 167 (1946) 550–595.
[43] C. Zener, Elasticity and anelasticity of metals, Chicago University Press, Illinois, USA, 1948.
[44] C. Zener, Physical Review 74 (1948) 639–647.
[45] R. A. Johnson, Acta Metallurgica 13 (1965) 1259–1262.
[46] H. K. D. H. Bhadeshia, Progress in Materials Science 57 (2012) 268–435.
[47] J. J. Bush, W. L. Grube, G. H. Robinson, ASM Transactions 54 (1961) 390–412.
[48] H. Swahn, P. C. Becker, O. Vingsbo, Metallurgical & Materials Transactions A 7 (1976) 35–39.
[49] R. Österlund, O. Vingsbo, Metallurgical & Materials Transactions A 11 (1980) 701–707.
[50] A. Marze, L. Vincent, B. Coquillet, J. Munier, P. Guiraldenq, Memoires Etudes Scientifiques Rev. Metallurg. 76 (1979) 165–173.
[51] J. H. Kang, Theory for mechanical tempering, 2013. Unpublished work, University of Cambridge.
[52] J. G. Speer, D. V. Edmonds, F. C. Rizzo, D. K. Matlock, Current Opinion in Solid State and Materials Science 8 (2004) 219–237.
[53] R. R. D. Avillez, E. S. D. Costa, A. R. F. A. Martins, G. C. Asuncao, International Journal of

Materials Research 99 (2008) 1280–1284.
[54] J. Mola, B. C. D. Cooman, Metallurgical & Materials Transactions A 65 (2012) 834–837.
[55] G. B. Olson, H. K. D. H. Bhadeshia, M. Cohen, Acta Metallurgica 37 (1989) 381–389.
[56] G. B. Olson, H. K. D. H. Bhadeshia, M. Cohen, Metallurgical & Materials Transactions A 21A (1990) 805–809.
[57] J. W. Christian, Materials Transactions, JIM 33 (1992) 208–214.